Effects of radiative loss on premixed planar flame propagation

Zheng Chen

State Key Laboratory for Turbulence and Complex Systems, College of Engineering,
Peking University, Beijing 100871, China

Corresponding author: Zheng Chen, Ph.D.
State Key Laboratory for Turbulence and Complex Systems
Department of Mechanics and Engineering Science,
College of Engineering, Peking University
Beijing 100871, China
Tel: +86-(10) 6276-6232
Email: cz@pku.edu.cn

Colloquium topic: Fire Research

Paper length (method 1):

Main Text:	word processor count	=	3189
Equations:	(28 line + 2) × (7.6 words/line) × (1 column)	=	228
References:	(40+2)×(2.3 lines/reference) × (7.6 words/line)	=	734
Figure Captions:	word processor count	=	173
Figure 1:	(58 mm+10) × (2.2 words/mm) × (2 column)	=	299
Figure 2:	(53 mm+10) × (2.2 words/mm) × (2 column)	=	277
Figure 3:	(53 mm+10) × (2.2 words/mm) × (1 column)	=	138
Figure 4:	(74 mm+10) × (2.2 words/mm) × (1 column)	=	184
Figure 5:	(89 mm+10) × (2.2 words/mm) × (1 column)	=	217
Figure 6:	(73 mm+10) × (2.2 words/mm) × (1 column)	=	182
Figure 7:	(72 mm+10) × (2.2 words/mm) × (1 column)	=	180
Figure 8:	(53 mm+10) × (2.2 words/mm) × (2 column)	=	277
	Total	**=**	**6078 words**

Supplementary Material: no

Color reproduction: no (all color figures are to be printed in gray scale)

Effects of radiative loss on premixed planar flame propagation

Zheng Chen*

State Key Laboratory for Turbulence and Complex Systems, College of Engineering, Peking University, Beijing 100871, China

Abstract

Radiation is an important factor in fires. It can greatly affect large-scale flame propagation occurring in fire or explosion accidents, e.g., the flame propagating in a tunnel in the mining industry. In this study, theoretical analysis is conducted for the premixed planar flame propagation in an infinitely large domain with radiative loss. The emphasis is on the radiation-induced flow and its influence on flame propagation speed. Based on the assumptions of one-step chemistry, quasi-steady flame propagation and linear heat loss, expressions describing the change of laminar burning flux, flame propagation speed, and flame temperature with the flame position are derived. Analytical expression for flow speed is also obtained. The analytical results quantify the radiation-induced thermal and flow effects on small and large scale premixed flame propagation. It is found that the laminar burning flux and flame temperature are only affected by the radiation-induced thermal effect, while the influence on flame propagation speed is sequentially dominated by the radiation-induced thermal and flow effects. Furthermore, the theoretical results are validated by transient numerical simulations considering detailed chemistry and quartic radiative loss. Both theoretical and numerical results indicate that in fire or explosion accidents, the large-scale premixed flame propagation could be decelerated by the radiation-induced flow effect by a factor of the expansion ratio.

Keywords: Radiative loss, premixed flame, propagation speed, radiation-induced flow

* Corresponding author. E-mail: cz@pku.edu.cn

1. Introduction

It is well known that thermal radiation is an important factor in fire phenomena [1]. Accidental ignition, flame propagation, fire spread, and wildland fires can be greatly affected by radiation (e.g., [2-6]). In fires with very large length scales, radiation is the dominant mode of heat transfer [7]. However, in small-scale fires/flames, convection and conduction usually dominate while radiation becomes crucial only for mixtures near their flammability limits [7, 8]. The flammability limit, which is important in fire safety (e.g., [9]), is in fact determined by radiative loss for unstretched premixed planar flames [10]; and it can be affected by the interaction between thermal radiation and flame stretch/curvature [11-13]. However, for small-scale flames in mixtures far away from the flammability limits or even close to the stoichiometric ratio, thermal radiation has little influence on flame propagation speed and can be neglected [14].

For premixed flame propagation occurring in fire or explosion accidents (e.g., flame propagating in a tunnel in the mining industry [15, 16]), its propagation speed can be reduced by thermal radiation in two ways: (1) the flame temperature and thus the reactivity decreases due to radiative loss; and (2) the counter flow of burned gas generated by radiation cooling slows the flame propagation [17]. The former is referred to as the radiation-induced thermal effect, while the latter is the radiation-induced flow effect [14, 17]. In mixtures far away from their flammability limits, both effects are negligible for small-scale (~1 cm) flame propagation [18]. However, as shall be shown in this study, the radiation-induced flow effect has great impact on large-scale (~1 m) flame propagation.

In our previous study [18], large-scale premixed spherical flame propagation in a near-stoichiometric methane/air mixture was simulated. Such large-scale premixed spherical flame experiments were conducted in modern fire research [19-23]. It was found that radiation has little influence on the flame propagation speed when the flame radius is

below 4 cm. However, for large-scale spherical flame propagation with radius up to 4 m, the flame propagation speed can be reduced by two thirds due to the radiation-induced flow. Therefore, the radiation-induced flow has great impact on large-scale premixed flame propagation. Though numerical simulation in is helpful for understating the radiation effects on large-scale flame propagation, it is limited to specific fuel/air mixtures at specific conditions (initial temperature, pressure, and equivalence ratio) and has high computational cost. Moreover, numerical simulation cannot provide general expressions describing the radiation-induced flow and its effect on flame propagation speed, which are important for fire safety control. Though there are many theoretical studies on how radiation affects flame quenching and flammability limits (e.g., [8] and references therein), there is no theoretical work on radiation-induced flow and its influence on premixed flame propagation.

Based on the above-mentioned considerations, the objectives of this study are to provide a general theoretical description of premixed flame propagation in an infinitely large domain with radiative loss, and to investigate how the radiation-induced flow affects large-scale flame propagation. In the following sections, the mathematical model and theoretical analysis are introduced first. Then, the results based on analytical solutions are presented and the radiation effects are assessed. Finally, numerical simulations without assumptions used in theoretical analysis are performed to validate the theoretical results.

2. Theoretical analysis

As shown in Fig. 1, we consider a simplified model of one-dimensional, premixed, planar flame propagation with radiative loss. Ignition at the symmetric plane results in two planar flames propagating in the opposite directions. The burned gas at the center (i.e., x=0) has the lowest temperature of T_0 since it has the longest radiation time. Due to the symmetry, we only need consider the flame propagating to the right with $x\geq 0$. This mimics

a premixed flame propagating from the closed end of a long tunnel, which might occur in fire or explosion accidents.

It is noted that the present model is only applicable for unstretched laminar flames in domains of infinite extend in the vertical direction. When the domain height is finite, the heat loss at the boundaries is different from that at the domain center and the present model cannot be used. This is one of the limitations of the present model.

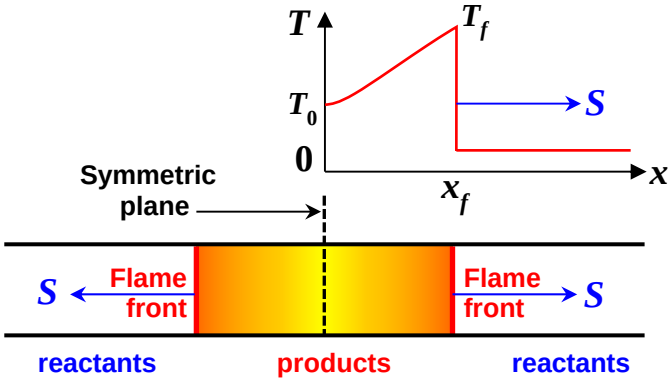

Fig. 1 Schematic premixed planar flame propagation with radiative loss.

Since the premixed flame propagates at a very low Mach number in an open space, constant pressure can be assumed and thereby the momentum equation needs not to be solved. Therefore, we only need consider the following non-dimensional equations for mass conservation, temperature and fuel mass fraction:

$$\frac{\partial \rho}{\partial t}+\frac{\partial}{\partial x}(\rho u)=0 \tag{1}$$

$$\rho\left(\frac{\partial T}{\partial t}+u\frac{\partial T}{\partial x}\right)=\frac{\partial^2 T}{\partial x^2}-H+\omega \tag{2}$$

$$\rho\left(\frac{\partial Y}{\partial t}+u\frac{\partial Y}{\partial x}\right)=\frac{1}{Le}\frac{\partial^2 Y}{\partial x^2}-\omega \tag{3}$$

where t, x, ρ, u, T, Y, H, and ω are the non-dimensional time, spatial coordinate, density, flow speed, temperature, fuel mass fraction, heat loss and reaction rate, respectively. Their relations to the dimensional counterparts are

$$t=\frac{\tilde{t}}{\tilde{\delta}_f^0/\tilde{S}_L^0},\ x=\frac{\tilde{x}}{\tilde{\delta}_f^0},\ \rho=\frac{\tilde{\rho}}{\tilde{\rho}_u},\ u=\frac{\tilde{u}}{\tilde{S}_L^0},\ T=\frac{\tilde{T}-\tilde{T}_u}{\tilde{T}_{ad}-\tilde{T}_u},\ Y=\frac{\tilde{Y}}{\tilde{Y}_u},$$

$$H=\frac{\tilde{H}\tilde{\delta}_f^0}{\tilde{\rho}_u\tilde{C}_P\tilde{S}_L^0(\tilde{T}_{ad}-\tilde{T}_u)},\ \omega=\frac{\tilde{\omega}\tilde{\delta}_f^0}{\tilde{\rho}_u\tilde{S}_L^0\tilde{Y}_u} \tag{4}$$

The parameters with and without ~ denote the dimensional and non-dimensional variables, respectively. In Eq. (4), $\tilde{\rho}_u$, $\tilde{T}_u$ and $\tilde{Y}_u$ denote the density, temperature and fuel mass fraction of the unburned mixture, respectively. $\tilde{T}_{ad}$, $\tilde{S}_L^0$ and $\tilde{\delta}_f^0$ are respectively the flame temperature, laminar flame speed and flame thickness of an adiabatic planar flame. The Lewis number is the ratio between thermal diffusivity of the mixture and fuel mass diffusivity, i.e., $Le=\tilde{\alpha}/\tilde{D}_F$. The reaction rate for a one-step irreversible reaction is $\tilde{\omega}=\tilde{\rho}\tilde{A}\tilde{Y}\exp(-\tilde{E}/\tilde{R}^0\tilde{T})$, in which $\tilde{A}$ is the pre-factor of the Arrhenius law, $\tilde{E}$ the activation energy, and $\tilde{R}^0$ the universal gas constant. The volumetric radiative loss is $\tilde{H}$.

In the coordinate attached to the moving flame front, the flame propagation can be considered as in a quasi-steady state. This quasi-steady assumption has been widely used in previous studies [12, 24-27] and validated by transient numerical simulations [12, 27]. Consequently, the governing equations are simplified to

$$-S\frac{d\rho}{dx}+\frac{d}{dx}(\rho u)=0 \tag{5}$$

$$\rho(u-S)\frac{dT}{dx}=\frac{d^2T}{dx^2}-hT+\omega \tag{6}$$

$$\rho(u-S)\frac{dY}{dx}=\frac{1}{Le}\frac{d^2Y}{dx^2}-\omega \tag{7}$$

where S is the flame propagation speed, i.e., $S=S(x_f)=dx_f/dt$. For mathematical simplicity, the heat loss is approximated as a linear function of temperature, $H=hT$, in which h is the heat loss intensity. As shown in [28], the linear and quartic radiative loss models have

qualitatively and even quantitatively similar influence on flame propagation when the heat loss intensities are properly specified. This is also confirmed by numerical simulations considering quartic radiative loss in Section 4. For real flames, the radiative loss intensity can be approximately determined according to Eq. (4). Another way is to numerically determine the radiative loss intensity under the requirement that the same normalized laminar flame speed is ensured for linear and quartic radiative loss models.

The non-dimensional boundary conditions are

$$x = 0: \quad dT/dx = dY/dx = u = 0 \tag{8}$$

$$x \to +\infty: \quad T = Y - 1 = du/dx = 0 \tag{9}$$

Integrating Eq. (5) with the zero flow speed boundary condition in Eq. (8) yields the following expression for laminar burning flux, m,

$$m = \rho(S - u) = \rho_0 S \tag{10}$$

where ρ_0 is the density at the center (x=0). Similar to S, ρ_0 and m both change with the flame position x_f.

In the limit of large activation energy, chemical reaction occurs only within a thin flame sheet at x=x_f [29, 30]. Outside of the flame sheet the flow can be considered to be chemically frozen (i.e. ω=0 in Eqs. 6 and 7) [29, 30]. With the help of Eq. (10) and the zero reaction rate outside the flame sheet, Eqs. (6) and (7) can be solved analytically. The solutions for the temperature and fuel mass fraction distributions are obtained as:

$$T(x) = \begin{cases} T_f \left[\dfrac{\lambda_2 \exp(\lambda_1 x) - \lambda_1 \exp(\lambda_2 x)}{\lambda_2 \exp(\lambda_1 x_f) - \lambda_1 \exp(\lambda_2 x_f)} \right] & \text{for} \quad 0 \le x \le x_f \\ T_f \exp[\lambda_2 (x - x_f)] & \text{for} \quad x \ge x_f \end{cases} \tag{11}$$

$$Y(x) = \begin{cases} 0 & \text{for} \quad 0 \le x \le x_f \\ 1 - \exp[-mLe(x - x_f)] & \text{for} \quad x \ge x_f \end{cases} \tag{12}$$

where T_f is the flame temperature to be determined and $\lambda_{1,2} = (-m \pm \sqrt{m^2 + 4h})/2$.

According to the asymptotic analysis in [29, 30], the following jump conditions hold across the flame front (x=x_f):

$$\left.\frac{dT}{dx}\right|_{x_f^-} - \left.\frac{dT}{dx}\right|_{x_f^+} = \frac{1}{Le}\left(\left.\frac{dY}{dx}\right|_{x_f^+} - \left.\frac{dY}{dx}\right|_{x_f^-}\right) = [(1-\sigma)T_f + \sigma]^2 \exp\left[\frac{Z}{2}\cdot\frac{T_f - 1}{(1-\sigma)T_f + \sigma}\right] \tag{13}$$

where σ is the thermal expansion ratio (which is equal to the ratio between the initial temperature and adiabatic flame temperature) and Z is the Zel'dovich number.

Substituting Eqs. (11) and (12) into (13) yields the following expressions among the laminar burning flux m, flame temperature T_f and flame position x_f:

$$T_f(\lambda_1 - \lambda_2)/[1 - \frac{\lambda_1}{\lambda_2}e^{(\lambda_2 - \lambda_1)x_f}] = m = [(1-\sigma)T_f + \sigma]^2 \exp\left[\frac{Z}{2}\frac{T_f - 1}{\sigma + (1-\sigma)T_f}\right] \tag{14}$$

For given values of h, σ and Z, the change of laminar burning flux m and flame temperature T_f with the flame position x_f can be obtained by solving the above algebraic equations. In the limit of $x_f \to \infty$, Eq. (14) recovers the classical theory on flammability limit for planar flames in an infinitely large domain [29]

$$(S^0)^2 \ln[(S^0)^2] = -2hZ \tag{15}$$

where S^0 denotes the non-dimensional planar flame speed or laminar burning flux.

The temperature at the center, T_0, is obtained from Eq. (11) at x=0:

$$T_0 = T(x=0) = T_f(\lambda_2 - \lambda_1)/[\lambda_2 \exp(\lambda_1 x_f) - \lambda_1 \exp(\lambda_2 x_f)] \tag{16}$$

The density at the center (x=0), ρ_0, can be obtained from the non-dimensional equation of state

$$\rho = \frac{1}{(\sigma^{-1} - 1)T + 1} \tag{17}$$

According to Eq. (10), we have the following expressions for the flame propagation speed and flow speed:

$$S = [T_0(\sigma^{-1} - 1) + 1]m \tag{18}$$

$$u = (\rho_0^{-1} - \rho^{-1})m = (T_0 - T)(\sigma^{-1} - 1)m \tag{19}$$

Equation (19) indicates that the maximum and minimum flow speeds occur, respectively, in the unburned gas with lowest temperature of T=0 and in the burned gas with the highest temperature of T=T_f

$$u_{\max} = T_0(\sigma^{-1} - 1)m\,, \quad u_{\min} = (T_0 - T_f)(\sigma^{-1} - 1)m \tag{20}$$

It is noted that in the present model, the density is not assumed to be constant. Consequently, the thermal expansion induced flow and radiation-induced flow are both considered and obtained as in Eq. (19).

3. Results and discussion

In this section, the results based on analytical solutions given by Eqs. (11-20) are presented. The expansion ratio (equal to the temperature ratio since the pressure is constant) and Zel'dovich number are fixed to be σ=0.15 and Z=10, respectively. These are typical values for premixed hydrocarbon/air flames.

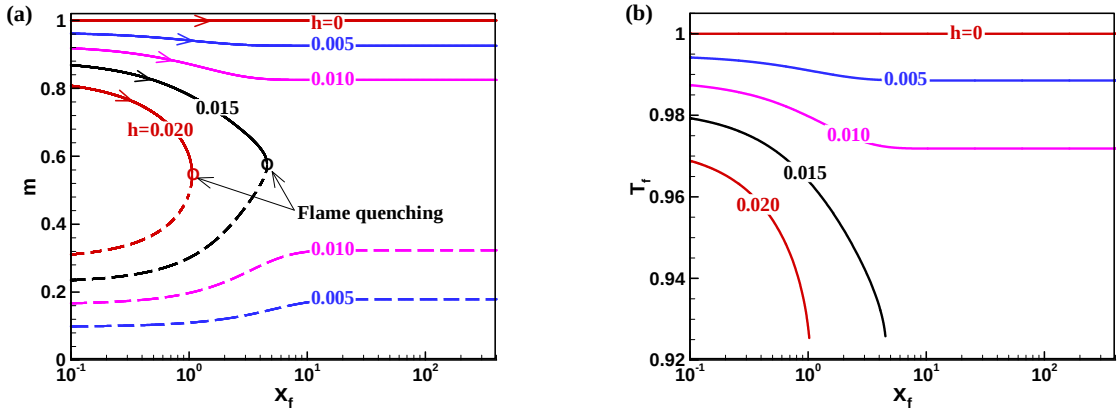

Fig. 2 Change of (a) the laminar burning flux, m, and (b) flame temperature, T_f, with flame position, x_f, at different radiative loss intensities.

Figure 2 shows the effects of radiative loss on the laminar burning flux and flame temperature. For each radiative loss intensity h>0, there are two branches in the m-x_f plot in Fig. 2(a). Physical flame propagation can occur only for the upper branch (solid lines);

while the lower branch represents unstable solutions (dashed lines) [29]. Only the upper branches are shown in the T_f-x_f plot in Fig. 2(b). At relatively large heat loss intensities of h=0.015 and 0.02 which are out of the flammability limit, the flame can propagate at relative small x_f. Here x_f is equal to the length of the radiating burned zone. Therefore, the total radiative loss increases with x_f and it can quench the flame at some critical value of x_f. This phenomenon is similar to the self-extinguishing flame (SEF) observed by Ronney et al. [31] in micro-gravity conditions. However, the SEF reported in [31] is a propagating spherical flame and it is mainly due to the competition between radiative loss and stretch rate, both of which change with flame radius. Here the planar flame has zero stretch rate. Nevertheless, it is difficult to obtain a planar SEF since the critical value of x_f shown in Fig. 2(a) is small. It is noted that in theory ignition is not considered and the initial flame is assumed to already appear. In practice, the insufficient ignition energy can result in flame kernel quenching. However, flame extinction reported in this work is not due to insufficient ignition energy, but due to radiation loss.

Figure 2 shows that both m and T_f decrease with the flame position for x_f<10; while they remain nearly constant for x_f>10. This is unlike the change of flame propagation speed with flame position as shown in Fig. 3.

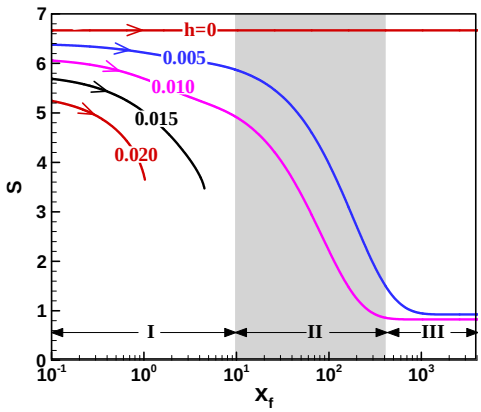

Fig. 3 Flame propagation speed as a function of the flame position at different radiative loss intensities.

Figure 3 shows that for the adiabatic case (h=0), the flame propagates at a constant speed. The speed is S=1/σ=6.67 rather than S=1. This is because the burned gas is static and thereby S is the flame speed relative to the burned gas. For h=0.005 and 0.010, three regions in terms of the flame position are observed. In region I, the flame propagation speed slightly decreases from the value of S=m/σ; while in region III it approaches to the constant value of S=m (the value for m is shown in Fig. 2a). Region II is a transition between regions I and III, in which the flame propagation speed S decreases from S=m/σ to S=m, i.e., by a factor of 1/σ. This is due to the negative flow speed, u_{min} in Eq. (20), induced by radiation cooling of burned gas. As shown in [14, 17, 32], radiation has two effects on flame propagation: (1) the radiation-induced thermal effect by which the flame temperature and thus flame propagation speed are reduced; and (2) the radiation-induced flow effect by which flame propagation speed is reduced due to the negative flow of burned gas caused by radiation cooling. The laminar burning flux and flame temperature shown in Fig. 2 are only affected by the radiation-induced thermal effect. However, the flame propagation speed shown in Fig. 3 is influenced by both radiation-induced thermal and flow effects. This is demonstrated by results in Figs. 4 and 5.

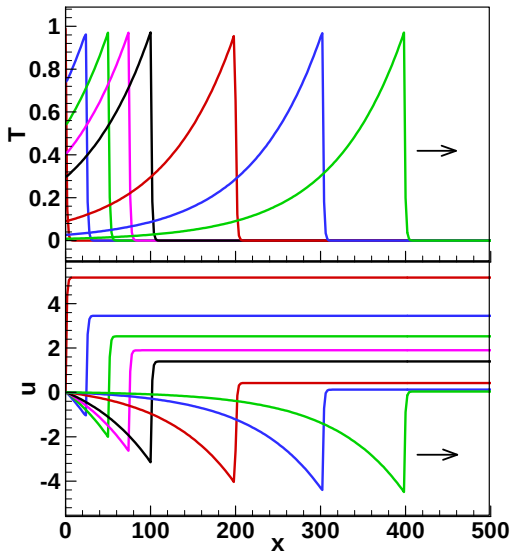

Fig. 4 Evolution of temperature and flow speed distributions during premixed flame

propagation with h=0.01. Note the time difference between two neighboring lines is not constant.

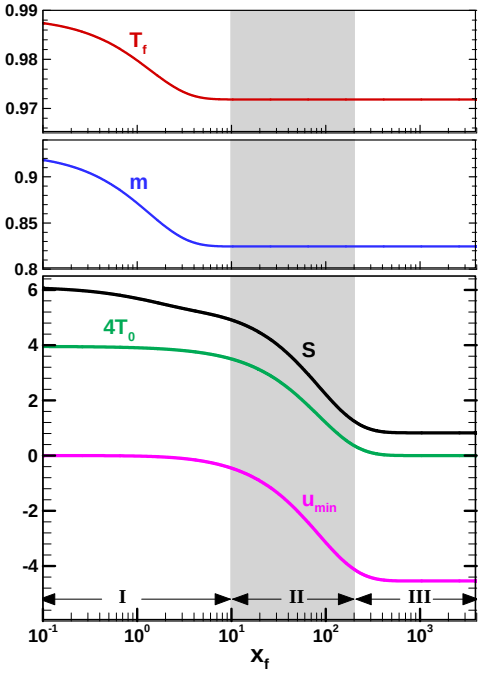

Fig. 5 Change of different velocities and temperatures with the flame position for h=0.01.

Figure 4 shows that opposite to the direction of flame propagation, the burned gas moves to the left and has negative flow speed. The absolute value of the burned gas speed increases significantly when the flame propagates from x_f=10 to x_f=100. This explains the sharp decrease of flame propagation speed in region II as shown in Fig. 3. The negative burned gas speed is due to the continuously decrease of burned gas temperature caused by radiation cooling. In region I (x_f<10), the burned gas is nearly static and thereby S is the flame speed relative to the burned gas. While in region III (x_f>400), the unburned gas is nearly static (see Fig. 4b) and thus S is the flame speed relative to the unburned gas. This further explains why the propagation speed S decreases by a factor of $1/\sigma$ from region I (where $S=m/\sigma$) to region III (where $S=m$).

Figures 4 and 5 shows that the flame temperature T_f remains nearly constant while the temperature at the center, T_0, continuously decreases. Consequently, according to Eq.

(20) and as shown in Fig. 5, the value of u_{min} continuously decreases during the flame propagation. Therefore, Fig. 5 indicates that in regions II and III, the flame propagation speed is main influenced by the radiation-induced negative flow speed, u_{min}, and the radiation-induced thermal effect is negligible.

The relative change in flame propagation speed caused by radiation-induced thermal and flow effects can be quantified, respectively, by a_{therm} and a_{flow}:

$$a_{therm} = 1 - \sigma(S - u_{\min}), \quad a_{flow} = -\sigma u_{\min} \tag{21}$$

The radiation-induced thermal and flow effects on flame propagation speed are shown in Fig. 6. For h=0.015 and 0.02, the thermal effect dominates over the flow effect before flame quenching occurs (see Fig. 2). For h=0.005 and 0.01, the thermal effect dominates over the flow effect for x_f <10. However, when the flame propagates from x_f =10 to x_f=200, the flow effect increases substantially in region II. Eventually, the flow effect dominates over the thermal effect in region III. Therefore, the flame propagation is sequentially affected by the radiation-induced thermal and flow effects. For large flame position, the flame propagation is slowed down by a factor of $1/\sigma$ (in the range of 4~7) due to the radiation-induced flow effect. Accordingly, in fire or explosion accidents, the large-scale premixed flame propagation could be decelerated by the radiation-induced flow effect, which reduces the propagation speed by a factor of $1/\sigma$.

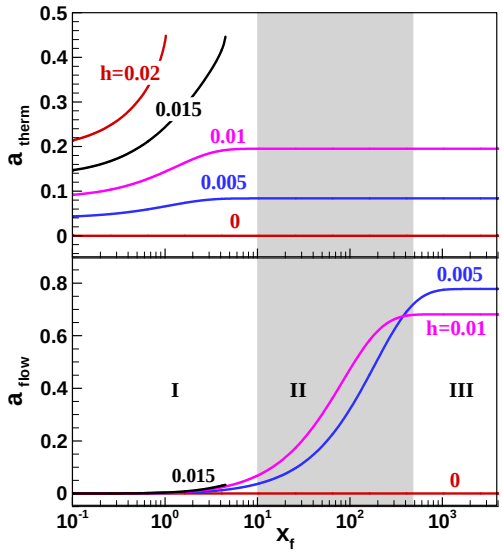

Fig. 6 Change of the radiation-induced thermal and flow effects on the flame propagation speed with the flame position at different radiative loss intensities.

4. Numerical validation

The above theoretical analysis is based on the assumptions of one-step chemistry, quasi-steady flame propagation and linear heat loss. To validate the theoretical results, transient simulations of 1D premixed stoichiometric CH_4/air flames are conducted by using the in-house code A-SURF [17, 33, 34]. Finite volume method is used to numerically solve the conservation equations for compressible reactive flow with multi species. The CHEMKIN package [35] is incorporated into A-SURF to calculate the thermal and transport properties and reaction rates. The detailed chemistry, GRI Mech. 3.0 [36], is considered. The mixture-averaged model is used to calculate the mass diffusivities of all species. For radiative loss, the optically thin model is used and the radiation emission from CO_2, H_2O, CO, and CH_4 is considered [37]. The detailed description of governing equations and numerical methods can be found in [17, 33, 34].

In simulation we consider the same model as the one shown in Fig. 1. The computational domain is $0 \le x \le 10$ m. Adaptive mesh refinement with the smallest mesh size of 32 μm is used to efficiently resolve the flame propagation in such an extremely

large computational domain (see Fig. 1 in [18]). Same as those in the theoretical analysis, symmetrical and transmissive boundaries are used at x=0 m and x=10 m, respectively. Flame propagation is initiated by a hot spot with the width of 2 mm around x=0 m.

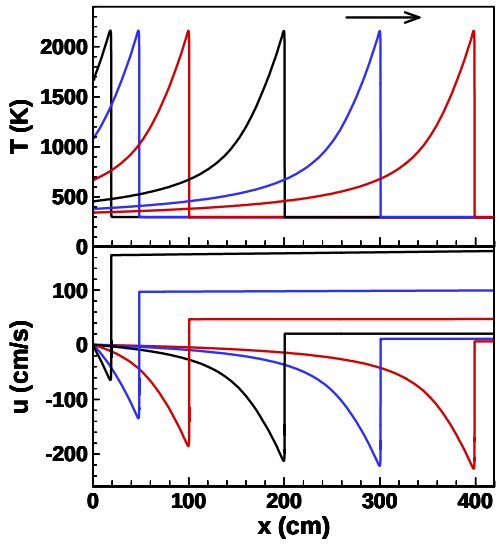

Fig. 7 Evolution of temperature and flow speed distributions during a premixed planar flame propagating in a stoichiometric CH_4/air mixture at 298 K and 1 atm.

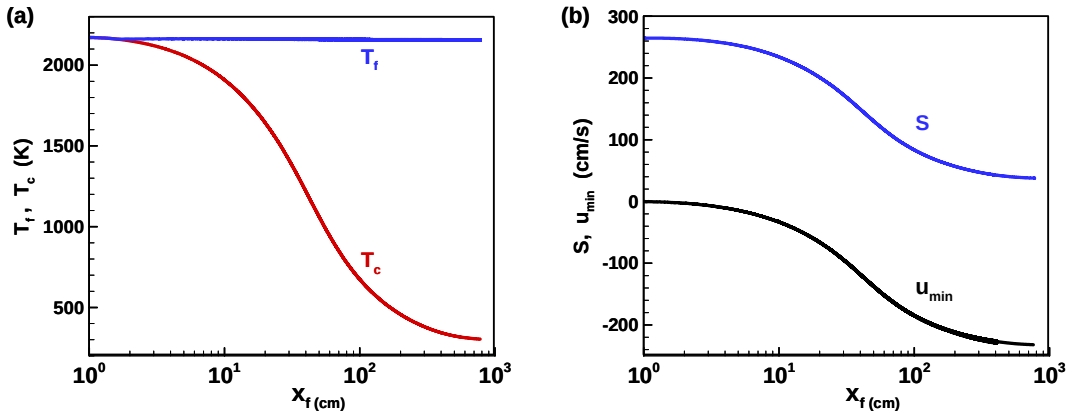

Fig. 8 Change of flame temperature, T_f, temperature at the center, T_c, flame propagation speed, S, and minimum flow speed, u_{min}, with the flame position, x_f, during a premixed planar flame propagating in a stoichiometric CH_4/air mixture at 298 K and 1 atm.

Figures 7 and 8 shows the simulation results. The temperature of burned gas is shown to continuously decrease, which results in the negative flow speed of burned gas as shown Fig. 7. These results are qualitatively similar to theoretical results shown in Fig. 4. Besides, Fig. 8 shows that the flame temperature remains near constant while the temperature at the

center continuously decreases and eventually drops to the ambient temperature of 298 K. The flame propagation speed S continuously decreases due to the negative flow speed, u_{min}, caused by radiation cooling. These results are similar to theoretical results shown in Fig. 5.

Therefore, the transient numerical simulations considering detailed chemistry and quartic radiative loss qualitatively validate the theoretical results, which are obtained under the assumptions of one-step chemistry, quasi-steady flame propagation and linear heat loss.

5. Conclusions

Theoretical analysis is conducted for one-dimensional premixed planar flame propagation with radiative loss. Expressions describing the change of laminar burning flux, flame propagation speed, and flame temperature with the flame position, Eq. (14), are derived. Analytical expression for flow speed, Eq. (19), is also obtained. Based on the analytical solutions, the effects of radiative loss on premixed planar flame propagation are assessed. It is found that the self-extinguishing flame can even happen to non-stretched premixed planar flames. The laminar burning flux and flame temperature are only affected by the radiation-induced thermal effect. However, the flame propagation speed is influenced by both the radiation-induced thermal and flow effects: the thermal effect dominates over the flow effect at the beginning, while the flow effect increases substantially during flame propagation and eventually it dominates over the thermal effect. The present analysis indicates that in fire or explosion phenomena, the large-scale premixed flame propagation can be decelerated greatly by the radiation-induced flow effect. The propagation speed can be reduced by a factor of $1/\sigma$ (in the range of 4~7).

Transient numerical simulations considering detailed chemistry and the radiation emission from CO_2, H_2O, CO, and CH_4 are conducted for 1D stoichiometric CH_4/air flame propagating in an extremely large computational domain. The simulation results confirm

the validity of theoretical analysis.

It is noted that here a simplified ideal model neglecting stretch and turbulence is considered so that analytical solutions can be derived. In practical fire or explosion events, usually the premixed flame is not planar or laminar. It can accelerate due to flame instability or turbulent flow. Nevertheless, radiation still has great impact on such large-scale premixed flame propagation [18], and the present theory can still be used to interpret the radiation-induced thermal and flow effects. Besides, radiative preheating of unburned reactants due to radiation reabsorption can accelerate flame propagation and even trigger deflagration to detonation transition [37-40]. This is not included in the present theory and it deserves further study.

Acknowledgments

This work was supported by National Natural Science Foundation of China (Nos. 91841302 and 91741126).

References

[1] D. Drysdale, An Introduction to Fire Dynamics, John Wiley and Sons, New York, 1999.

[2] B.W. Butler, M.A. Finney, P.L. Andrews, F.A. Albini, A radiation-driven model for crown fire spread, Can. J. Forest Res. 34 (2004) 1588-1599.

[3] G. Linteris, M. Zammarano, B. Wilthan, L. Hanssen, Absorption and reflection of infrared radiation by polymers in fire-like environments, Fire Mater. 36 (2012) 537-553.

[4] A. Palacios, M. Munoz, R. M. Darbra, J. Casal, Thermal radiation from vertical jet fires, Fire Safety J. (2012) 93-101.

[5] P.F. Wang, N.A. Liu, Y.L. Bai, L.H. Zhang, K. Satoh, X.Y. Liu, An experimental study on thermal radiation of fire whirl, Int. J. Wildland Fire 26 (2017) 693-705.

[6] L. Zhou, D. Zeng, D. Y. Li, M. Chaos, Total radiative heat loss and radiation distribution of liquid pool fire flames, Fire Safety J. 89 (2017) 16-21.

[7] J. Ris, Fire radiation—a review, Proc. Combust. Inst. 17 (1979).

[8] Y. Ju, K. Maruta, T. Niioka, Combustion limits, Applied Mech. Rev. 54 (2001) 257-277.

[9] C.V. Mashuga, D.A. Crowl, Application of the flammability diagram for evaluation of fire and explosion hazards of flammable vapors, Process Safety Prog. 17 (1998) 176-183.

[10] D. B. Spalding, A theory of inflammability limits and flame-quenching, Proceedings of the Royal Society of London. Ser. A Math. Phys. Eng. Sci., 240 (1957) 83-100.

[11] Z. Chen, Y. Ju, Combined effects of curvature, radiation, and stretch on the extinction of premixed tubular flames, Int. J. Heat Mass Transfer 51 (2008) 6118-6125.

[12] Z. Chen, Y. Ju, Theoretical analysis of the evolution from ignition kernel to flame ball and planar flame, Combust. Theory Model. 11 (2007) 427-453.

[13] H.W. Zhang, Z. Chen, Bifurcation and extinction limit of stretched premixed flames with chain-branching intermediate kinetics and radiative loss, Combust. Theory Model. 22 (2018) 531-553.

[14] H. Yu, W. Han, J. Santner, X. Gou, C.H. Sohn, Y. Ju, Z. Chen, Radiation-induced uncertainty in laminar flame speed measured from propagating spherical flames, Combust. Flame 161 (2014) 2815-2824

[15] S. Demir, V. Bychkov, S.H.R. Chalagalla, V. Akkerman, Towards a predictive scenario of a burning accident in a mining passage, Combust. Theory Model. 21 (2017) 997-1022.

[16] E. Byrne, K. Georgieva, R. Carvel, Fires in Ducts: A review of the early research which underpins modern tunnel fire safety engineering, Tunn. Undergr. Sp. Tech. 81 (2018) 306-314.

[17] Z. Chen, Effects of radiation and compression on propagating spherical flames of methane/air mixtures near the lean flammability limit, Combust. Flame 157 (2010) 2267-2276.

[18] Z. Chen, Effects of radiation on large-scale spherical flame propagation, Combust. Flame 183 (2017) 66-74.

[19] D. Bradley, T.M. Cresswell, J.S. Puttock, Flame acceleration due to flame-induced instabilities in large-scale explosions, Combust. Flame 124 (2001) 551-559.

[20] C.R. Bauwens, J.M. Bergthorson, S.B. Dorofeev, Experimental study of spherical-flame acceleration mechanisms in large-scale propane-air flames, Proc. Combust. Inst. 35 (2015) 2059-2066.

[21] W.K.Kim, T. Mogi, K. Kuwana, R. Dobashi, Self-similar propagation of

expanding spherical flames in large scale gas explosions, Proc. Combust. Inst. 35 (2015) 2051-2058.

[22] C.R. Bauwens, J.M. Bergthorson, S.B. Dorofeev, On the interaction of the Darrieus–Landau instability with weak initial turbulence, Proc. Combust. Inst. 36 (2017) 2815-2822.

[23] W. Kim, T. Endo, T. Mogi, K. Kuwana, R. Dobashi, Wrinkling of large-scale flame in lean propane-air mixture due to cellular instabilities, Combust. Sci. Techno. 191 (2019) 491-503.

[24] M.L. Frankel, G.I. Sivashinsky, On quenching of curved flames, Combust. Sci. Techno. 40 (1984) 257-268.

[25] M.L. Frankel, G.I. Sivashinsky, On effects due to thermal-expansion and Lewis number in spherical flame propagation, Combust. Sci. Techno. 31 (1983) 131-138.

[26] H. Zhang, Z. Chen, Spherical flame initiation and propagation with thermally sensitive intermediate kinetics, Combust. Flame 158 (2011) 1520-1531.

[27] H. Zhang, P. Guo, Z. Chen, Critical condition for the ignition of reactant mixture by radical deposition, Proc. Combust. Inst. 34 (2013) 3267-3275.

[28] H. Zhang, P. Guo, Z. Chen, Outwardly propagating spherical flames with thermally sensitive intermediate kinetics and radiative loss, Combust. Sci. Techno. 185 (2013) 226-248.

[29] G. Joulin, P. Clavin, Linear-stability analysis of non-adiabatic flames: diffusional-thermal model, Combust. Flame 35 (1979) 139-153.

[30] Y. Wu, Z. Chen, Asymptotic analysis of outwardly propagating spherical flames, Acta Mech. Sinica 28 (2012) 359-366.

[31] P. D. Ronney, On the mechanics of flame propagation limits and extinguishment processes at microgravity, Proc. Combust. Inst. 22 (1988) 1615-1623.

[32] Z. Chen, Effects of radiation absorption on spherical flame propagation and radiation-induced uncertainty in laminar flame speed measurement, Proc. Combust. Inst. 37 (2017) 1129-1136.

[33] Z. Chen, M.P. Burke, Y.G. Ju, Effects of Lewis number and ignition energy on the determination of laminar flame speed using propagating spherical flames, Proc. Combust. Inst. 32 (2009) 1253-1260.

[34] P. Dai, Z. Chen, Supersonic reaction front propagation initiated by a hot spot in n-heptane/air mixture with multistage ignition, Combust. Flame 162 (2015) 4183-4193.

[35] R.J. Kee, F. Rupley, J. Miller, CHEMKIN-II: A FORTRAN chemical kinetics

package for the analysis of gas-phase chemical kinetics, Sandia Report. SAND89-8009B (1993).

[36] G. Smith, D. Golden, M. Frenklach, The GRI-Mech 3.0 chemical kinetic mechanism. http://combustion.berkeley.edu/gri-mech/

[37] Z. Chen, X. Qin, B. Xu, Y.G. Ju, F.S. Liu, Studies of radiation absorption on flame speed and flammability limit of CO_2 diluted methane flames at elevated pressures, Proc. Combust. Inst. 31 (2007) 2693-2700.

[38] V. Karlin, Radiation preheating can trigger transition from deflagration to detonation, Flow Turbul. Combust. 87 (2011) 511-523.

[39] M.F. Ivanov, A.D. Kiverin, M.A. Liberman, Ignition of deflagration and detonation ahead of the flame due to radiative preheating of suspended micro particles, Combust. Flame 162 (2015) 3612-3621.

[40] M.A. Liberman, M.F. Ivanov, A.D. Kiverin, Effects of thermal radiation heat transfer on flame acceleration and transition to detonation in particle-cloud hydrogen flames, J. Loss Prevent. Proc. 38 (2015) 176-186.

Figure captions

Fig. 1 Schematic premixed planar flame propagation with radiative loss.

Fig. 2 Change of (a) the laminar burning flux, m, and (b) flame temperature, T_f, with flame position, x_f, at different radiative loss intensities.

Fig. 3 Flame propagation speed as a function of the flame position at different radiative loss intensities.

Fig. 4 Evolution of temperature and flow speed distributions during premixed flame propagation with h=0.01.

Fig. 5 Change of different velocities and temperatures with the flame position for h=0.01.

Fig. 6 Change of the radiation-induced thermal and flow effects on the flame propagation speed with the flame position at different radiative loss intensities.

Fig. 7 Evolution of temperature and flow speed distributions during a premixed planar flame propagating in a stoichiometric CH_4/air mixture at 298 K and 1 atm.

Fig. 8 Change of flame temperature, T_f, temperature at the center, T_c, flame propagation speed, S, and minimum flow speed, u_{min}, with the flame position, x_f, during a premixed planar flame propagating in a stoichiometric CH_4/air mixture at 298 K and 1 atm.